# MONTE CARLO SIMULATION OF PHOTON BREAST RADIOTHERAPY OF THE PREGNANT PATIENT
## Beam Characteristics

by

***Dario FAJ*** [1,2]***, Hrvoje BRKIĆ*** [1,2*]***, Vjekoslav KOPAČIN*** [1,3]***, Marija MAJER*** [4]***, Željka KNEŽEVIĆ*** [4]***, Svjetlana MARIĆ*** [2]***, and Mladen KASABAŠIĆ*** [1,3]

[1] Faculty of Medicine, Osijek, Croatia
[2] Faculty of Dental Medicine and Health, Osijek,Croatia
[3] Clinical Hospital, Osijek, Croatia
[4] Rudjer Bošković Institute, Zagreb, Croatia

Scientific paper
https://doi.org/10.2298/NTRP2402154F

**This paper aims to describe the photon beam characteristics in terms of energy and angular distribution during breast megavoltage photon radiotherapy of pregnant patients. Photon beam characteristics are investigated at treatment volume (breast) and the position of the fetus in the Tena phantom using Monte Carlo simulation. Photon beam energy spectra are compared across various materials used as substitutes for constructing physical and computational phantoms. Mean energies calculated in substitute materials developed by our group and used to build the Tena phantom, differ up to 10 % from the calculated ones in ICRU reference tissue materials. It was found acceptable since this is less than the differences between ICRP and ICRU materials. Then, the photon beam characteristics are investigated in the anthropomorphic phantom, Tena. Photon beam mean energy in the fetal region of the phantom (out-of-field) is significantly lower (more than 1 MeV) than at the breast position (in-field). The angular distribution of the photon beam at the breast position predominantly shows a forward direction, whereas, at the fetus position, the distribution is more scattered. When selecting a detector, it is crucial to consider the differences in photon energy and angular distributions between in-field and out-of-field measurement points to reduce measurement uncertainties and ensure reliable data.**

*Key words: megavolt photon beam radiotherapy, Monte Carlo, beam characteristic, out-of-field pregnant patient*

## INTRODUCTION

According to the FIGO 2018 report [1], the incidence of carcinoma during pregnancy is reported to be 1:1000-1:1500 pregnancies. The incidence has increased over the past 30 years [2]. With an incidence of 1:10000 up to 1:3000, breast carcinoma is the most common malignant tumor during pregnancy [3]. Radiotherapy (RT) of pregnant patients has drawn special attention from scientific and clinical communities in the past few years [3-5].

Techniques and data that can aid the medical physicist who needs to plan the radiation therapy of a pregnant patient using photon beams are given in several reports [6, 7]. It has been shown that treatment planning systems (TPS) ar not accurate in assessing out-of-field doses [8-10]. There are empirical methods for fetal dose estimation in photon radiotherapy based on measurements in simple geometry [7]. Measurements in phantoms or Monte Carlo (MC) simulations could give more accurate results, especially if patient anatomy is used close to the actual [3, 5]. Luminescent detectors, such as radio photoluminescent (RPL), thermoluminescent (TL), and optically stimulated luminescent (OSL) detectors, are widely used to measure photon out-of-filed doses in different phantoms during various RT procedures [11-15]. Detectors are commonly calibrated in the standard photon fields (such as $^{137}$Cs and $^{60}$Co gamma fields). However, out-of-field radiation is made of secondary/scattered radiation and there is a different energy and angular spectrum at various positions in phantoms. Therefore, correction for energy and angular dependence of TL, OSL, and RPL detectors should be applied if needed [11, 14]. In addition to luminescent detectors, other detectors such as films, diodes, ion chambers, and MOSFET are also used for out-of-field photon dosimetry [6]. To find out if corrections are needed for a de-

* Corresponding author, e-mail: hbrkic@mefos.hr

tector used for photon dosimetry, photon beam characteristics in terms of energy and angular distribution in measurement (fetal) positions for RT of interest should be known.

The MC simulations are a valuable research method since they can provide data beyond the experimental approach [16, 17]. However, their setup and computational time require significant effort. Additionally, MC simulations involve uncertainties, such as underestimating the absorbed dose outside the primary radiation field [18, 19].

This paper aims to describe the photon beam characteristics, specifically energy and angular distribution, during breast photon radiotherapy for a pregnant patient. The photon beam characteristics are presented in the treatment volume (breast) and the fetus position (outside the treatment field) using MC simulation of RT beams in an anthropomorphic phantom. These characteristics are compared across different materials used as substitutes for constructing physical or computational phantoms.

## MATERIALS AND METHODS

The MC simulation, of Siemens Oncor medical linear accelerator, was applied for the MV breast RT of the pregnant patient. The RT was simulated using the 3-D conformal RT technique with five beams (2 medial, 2 lateral, and one posterior). To obtain information that is beyond the experiment and TPS data, MC simulations were performed using Monte Carlo N-Particle transport code (MCNP) version 6.2 [20]. Previous publications of this research group extensively tested the model of the accelerator used [21-24]. The materials used for the MC of the accelerator and the materials for the phantom were taken from the Compendium of material composition data for radiation transport modeling [25] and our previous publication respectively [4]. The voxelized form of the pregnant female phantom Tena was taken from Kopačin *et al.* [3]. The ENDF/ B-VII (Evaluated Nuclear data file B-VII) [26] cross- section data libraries were used to perform the simulations. The accelerator model includes the target, primary collimator, flattening filter, multi-leaf collimator (with each of the 80 leaves modeled separately, as shown in fig. 1), and head cover. Each gantry position and field shape were modeled individually. The electrons impinging on the target had an energy of 6 MeV with a Gaussian spread of 3 %.

To test the photon beam characteristics, several sets of MC simulations were performed. Since physical and radiological characteristics (physical density, effective atomic number, and CT number) of Tena substitute materials are already proven as reliable [4], we additionally compared scattering properties with those commonly used in RT procedures (ICRP) and reference tissue materials (ICRU). Scattering properties are

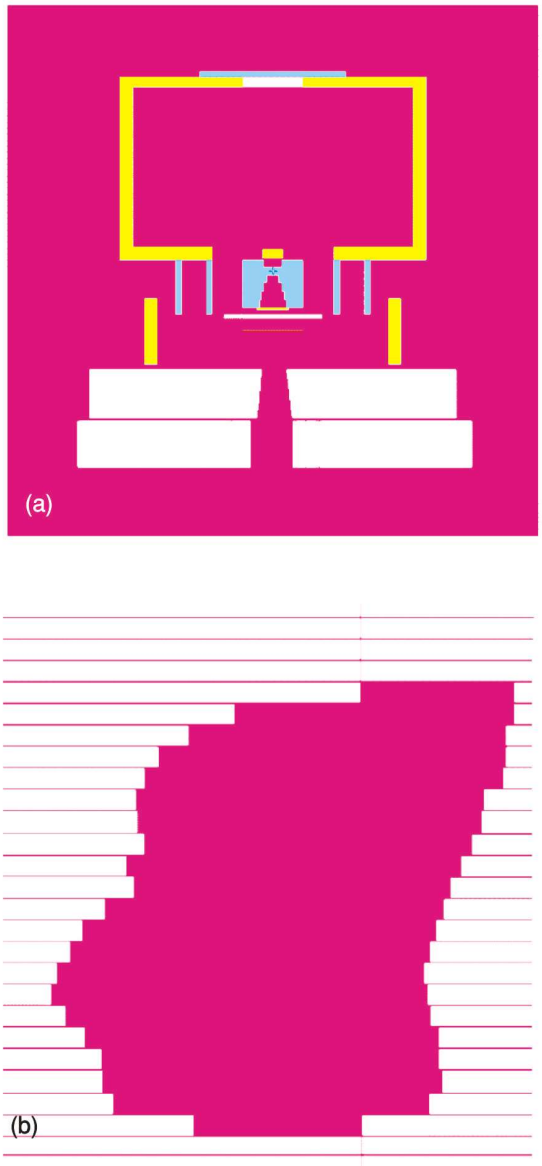


**Figure 1. The parts of the accelerator depicted using MCNP plotter accelerator head (a); position of the leaves forming the field F1 (b)**

tested using simplified MC simulations. Namely, the source was defined as isotropic with photon spectra obtained from previous simulations [3]. A box with dimensions of 30 cm × 30 cm × 30 cm was placed 90 cm from the isotropic source. The box for scoring spectra (5 cm × 5 cm × 0.2 cm, where the depth was 0.2 cm) was set at the depths of 5 cm and 10 cm. These depths are chosen as representative of the RT plan used in this work. Both larger box and detector boxes were filled with soft, lung and bone tissues that are defined by ICRP [27], ICRU [28], and Tena compositions [4]. In each simulation, $3 \cdot 10^9$ particles were simulated and an F4 tally was used to calculate the spectra in the detector boxes. The results were accepted if all 10 statistical checks for each tally were satisfied [29].

In the second set of simulations, the voxelized pregnant female phantom Tena was filled with Tena,

ICRU, and ICRP substitute materials. A full radiation therapy plan was applied to the phantom as defined in our earlier publications [3, 4]. The treatment plan consisted of only five fields, which were sufficient to cover the treatment volume. Such a small number of fields enabled us to easily incorporate field geometry into the MCNP input since each leaf needs to be positioned manually. Tallies for recording the spectra and angular distribution of the incident particles were positioned in cubes with a 1 cm base and overlapped with voxelized phantom geometry. The spectra were collected in the fetus's head (outside the treatment field) position and isocenter point, fig. 2. The distance between these two positions is 40 cm. Since the detector at the out-of-field position has a lower probability of sampling incident particles, to reduce the variance DXTRAN sphere with a 10 cm radius was set in the fetus' head. In this way, the number of particles that arrive at the detector increases. All the details regarding the simulations are described in the previous publication [4].

## RESULTS

In the first set of simulations MC simulations for the cube filled with each material, defined in three different ways (using ICRP material, ICRU material, and the Tena materials), were performed to estimate the mean energies at two different depths (5 cm and 10 cm, tab. 1). For soft tissue, mean energies correlate closely even for the depth of 10 cm, though for bone and lung tissue, the differences are larger. Relative errors of all simulations are below 0.1 %.

To choose appropriate dosimeters for measurements in the treatment volume and in the position of the fetus (second set of MC simulations) photon spectra were determined at both positions. All materials (Tena, ICRU, and ICRP) used in MC simulations show that spectra in treatment volume and outside the treatment field differ significantly figs. 3(a)-3(c). Error bars represent relative errors but since the error for most of the bins is below 1 % they are barely visible, especially in the breast position.

**Table 1. Mean energies at 5 cm and 10 cm depth in 30 cm × × 30 cm × 30 cm box filled with different tissue supplements as defined for ICRP, ICRU, and Tena materials**

| Material | Mean energy [MeV] | | | | | |
|---|---|---|---|---|---|---|
| | Bone | | Lung | | Soft tissue | |
| | 5 cm | 10 cm | 5 cm | 10 cm | 5 cm | 10 cm |
| TENA | 0.948 | 0.893 | 1.227 | 1.217 | 0.937 | 0.865 |
| ICRP | 0.864 | 0.789 | 0.921 | 0.848 | 0.935 | 0.863 |
| ICRU | 0.889 | 0.832 | 1.325 | 1.304 | 0.935 | 0.862 |

Photons at the fetus's position (outside the treatment field) showed a mean value of 0.3 MeV for Tena and ICRP materials, while ICRU has a mean energy of 0.45 MeV. In the treatment field, the mean values for ICRP, Tena, and ICRU are 1.53 MeV, 1.54 MeV, and 1.52 MeV, respectively. Figure 4 presents the angular distribution of photons in the breast and the position of the fetus during breast photon MV RT.

Angular distribution at the position of special interest (breast and position of the fetus) was also calculated in both positions. The probability of photon angle at the position of the fetus is marked in white while at the breast position is hatched. Error bars represent relative error. At 0° in each position (breast/fetus) the vector is directed from the accelerator target toward the treatment table at a gantry angle of 0°.

## DISCUSSIONS

Photon energies at two different depths in materials defined by ICRP, ICRU, and Tena physical phantom materials [3, 4] were investigated to additionally validate Tena substitute materials. Mean energies for these materials (ICRP, ICRU, and Tena), at two representative depths (5 cm and 10 cm) were examined. For bone material, Tena material composition overestimates the mean energies by approximately 7 % on both depths, while for lung tissue the dose is underestimated by 7 % when compared to ICRU materials. For soft tissue, the difference in mean energies is in the order of 0.3 %, even at greater depths, for all three materials. This is significant since most of the Tena phan-

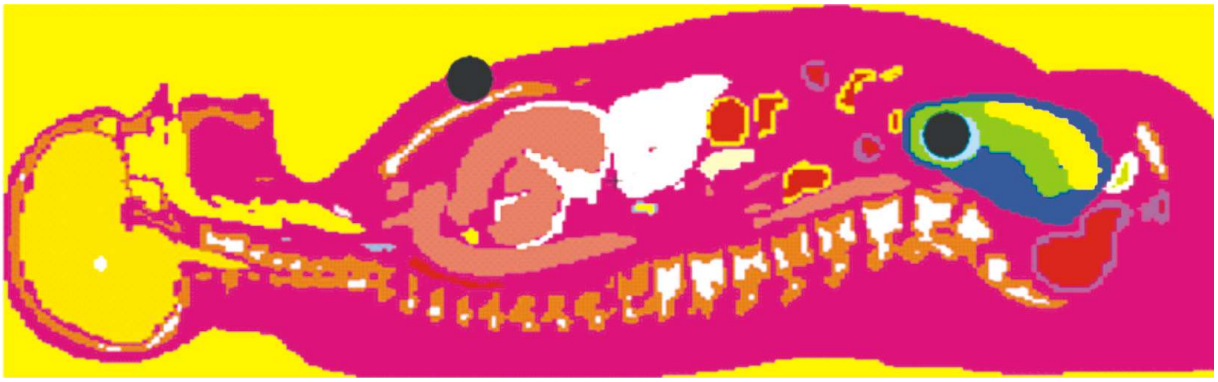

**Figure 2. Tena phantom with approximate positions of the detectors marked with black dots**

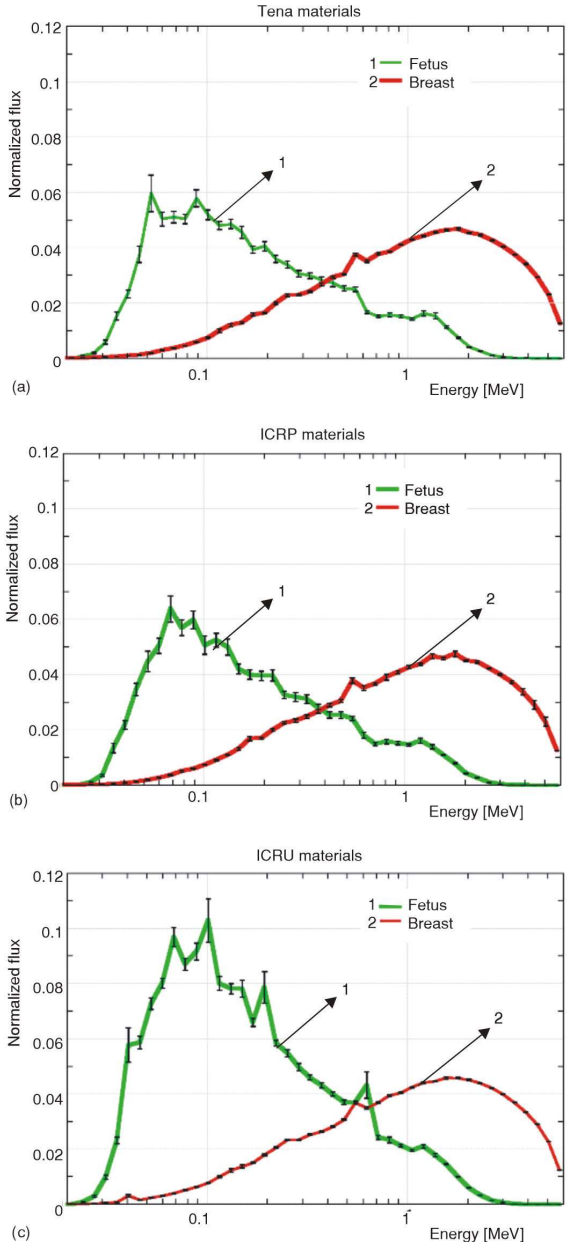


**Figure 3. Photon spectra at the breast and the position of the fetus for: Tena (a), ICRP (b), and ICRU material (c)**

tom is cast from the soft tissue substitute material. MC simulations showed better agreement of mean energies at 5 cm and 10 cm depth for Tena than for ICRP substitute materials when compared to ICRU reference material. This confirms the suitability of Tena substitute materials for RT beam dosimetry in the treatment volume.

The second part of the work was to determine photon beam characteristics in MV photon breast RT in treatment volume and the position of the fetus in the Tena phantom. Figure 3 shows photon energies at the treatment position and the position of the fetus in the Tena phantom for Tena, ICRP, and ICRU materials. A comparison of spectra and mean energies shows agreement in the treatment position as already shown with the previous set of MC simulations. Differences in photon spectra between Tena substitute material and ICRU reference material at the position of the fetus increase. Nevertheless, in the same position, photon spectra, as well as, photon mean energy in Tena substitute material are comparable to the ICRP substitute materials that are typically used for mathematical and physical phantom creation. Results shown in fig. 3 indicate significant differences in photon spectra between the treatment volume and position of the fetus in the Tena phantom. Similarly, fig. 4 shows large differences in the angular distribution of photons at these positions. Detectors that are widely used for measurements of photon out-of-field doses in RT, such as RPL, TL, and OSL, might need a correction factor due to changes in energy and angular spectrum at different positions in phantoms [11, 14, 15, 30]. This change comes because out-of-field radiation is made of scattered (secondary) radiation. Information on spectral or angular distribution and energy ranges, figs. 3(a)-3(c), or even the dose to the whole organ, is valuable information when choosing the appropriate detector for [10, 31]. The difference in mean energies at fetal (in-field) and breast (out-of-field) position, according to this study results, is more than 1 MeV, fig. 3, so the detectors of choice must be sensitive in both energy regions

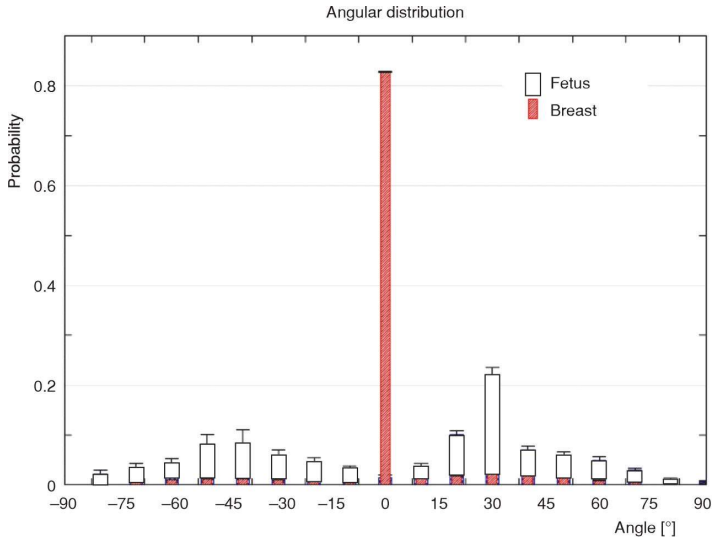


**Figure 4. Probability of photon angle at the breast and the position of the fetus during breast photon MV RT**

or appropriate correction factor must be applied. The data from our simulations showed that for the position of the fetus, only 3 % of all the particles impinging the detector have angles that are perpendicular to the initial beam, fig. 4, which is significantly different when compared to the particles inside the radiation field. These results are valuable for experiment setup since some of the detectors might show discrepancies if irradiated under these conditions [11, 30-32].

The TPS does not provide sufficient accuracy for dose calculations in regions far from the beam edge, as is the case with pregnant patients [33, 34]. However, for pregnant patients undergoing radiation therapy, the fetal dose is the crucial information needed for an optimal treatment process. Selecting the appropriate detector for estimating the dose at the position of the fetus, requires careful consideration of beam characteristics. This is essential for reducing measurement uncertainty and obtaining reliable data.

## CONCLUSION

The mean energies of Tena substitute materials differ up to 10 % from ICRU reference tissue materials. Photon mean energy in the fetal region (out-of-field) is significantly lower (more than 1 MeV) than at the breast position (in-field). At the position of the fetus, only 3 % of the particles impinging the detector have angles perpendicular to the initial beam. Differences in photon energy and angular distributions between in-field and out-of-field points of measurement need to be considered to decrease measurement uncertainties and obtain reliable measurement data.

## ACKNOWLEDGMENT

This work was financed by the EU-funded project SONORA - Towards safe, optimized, and personalized radiology and radiotherapy procedures for pregnant patients (PIANOFORTE HORIZON-EURATOM-2021-NRT-01-09) and institutional projects IP- MEFOS and IP FDMZ.

## AUTHORS' CONTRIBUTIONS

D. Faj conceived and designed the study and supervised the project; H. Brkić performed the simulations, prepared the graphics, and drafted the initial manuscript; V. Kopačin and M. Kasabašić interpreted the results and performed the data analysis; M. Majer, Ž. Knežević and S. Marić. critically reviewed the manuscript for important intellectual content.

All authors have read and approved the final version of the manuscript.

## ORCID NO

D. Faj: 0000-0002-4111-5459
H. Brkić: 0000-0001-6692-6875
V. Kopačin: 0000-0002-3854-6602
M. Majer: 0000-0002-0781-2365
Ž. Knežević: 0000-0001-6669-8788
M. Kasabašić: 0000-0002-6707-4317

## REFERENCES

[1] Bhatla, N., Denny, L., FIGO Cancer Report 2018, *International Journal of Gynecology & Obstetrics, 143* (2018), pp. 2-3
[2] Basta, P., *et al*., Cancer Treatment in Pregnant Women, *Contemporary Oncology, 19* (2015), 5, p. 354
[3] Kopačin, V., *et al*., Development of a Computational Pregnant Female Phantom and Calculation of Fetal Dose During a Photon Breast Radiotherapy, *Radiology and Oncology, 56* (2022), 4, pp. 541-551
[4] Kopačin, V., *et al*., Development and Validation of the Low-Cost Pregnant Female Physical Phantom for Fetal Dosimetry in MV Photon Radiotherapy, *Journal of Applied Clinical Medical Physics*, (2023)
[5] De Saint-Hubert, M., *et al*., Fetus Dose Calculation During Proton Therapy of Pregnant Phantoms Using MCNPX and MCNP6. 2 Codes, *Radiation Measurements, 149* (2021), 106665
[6] Kry, S. F., *et al*., AAPM TG 158: Measurement and Calculation of Doses Outside the Treated Volume from External-Beam Radiation Therapy, *Medical Physics, 44* (2017), 10, pp. e391-e429
[7] Stovall, M., *et al*., Fetal Dose from Radiotherapy with Photon Beams: Report of AAPM Radiation Therapy Committee Task Group No. 36, *Medical Physics, 22* (1995), 1, pp. 63-82
[8] Howell, R., *et al*., S.K.-P. in M.& and 2010, Undefined: Accuracy of Out-Of-Field Dose Calculations by a Commercial Treatment Planning System, *Iopscience.iop.org, 55* (2010), 23, 6999
[9] Majer, M., *et al*., Out-of-Field Doses in Pediatric Craniospinal Irradiations with 3D-CRT, VMAT, and Scanning Proton Radiotherapy: A Phantom Study, *Wiley Online Library, 49* (2022), 4, pp. 2672-2683
[10] Clouvas, A., *et al*., Capabilities of Electret Ion Chambers to Measure Absorbed Dose Outside the Treated Volume, During External-Photon Radiation Therapy, *Nucl Technol Radiat, 36* (2021), 2, pp. 197-204
[11] Bordy, J. M., *et al*., Radiotherapy Out-Of-Field Dosimetry: Experimental and Computational Results for Photons in a Water Tank, *Radiation Measurements, 57* (2013), pp. 29-34
[12] Miljanić, S., *et al*., Clinical Simulations of Prostate Radiotherapy Using BOMAB-Like Phantoms: Results for Photons, *Radiation Measurements, 57* (2013), pp. 35-47
[13] Stolarczyk, L., *et al*., Dose Distribution of Secondary Radiation in a Water Phantom for a Proton Pencil Beam-EURADOS WG9 Intercomparison Exercise, *Physics in Medicine & Biology, 63* (2018), 8, 085017
[14] De Saint-Hubert, M., *et al*., Out-Of-Field Doses in Children Treated for Large Arteriovenous Malformations Using Hypofractionated Gamma Knife Radiosurgery and Intensity-Modulated Radiation Therapy, *Radiation Protection Dosimetry, 181* (2018), 2, pp. 100-110
[15] Majer, M., *et al*., Out-Of-Field Dose Measurements for 3-D Conformal and Intensity Modulated Radio-

therapy of a Paediatric Brain Tumour, *Radiation Protection Dosimetry, 176* (2017), 3, pp. 331-340
[16] Pham, H., *et al*., Photon Beam Modeling, A Comparative Study of Primo and Gate Simulation Toolkits for the TrueBeam STx Linac, *Nucl Technol Radiat, 39* (2024), 1, pp. 58-65
[17] Tang, X., *et al*., Simulation and Measurement of X-Ray Scattered Radiation in Radiodiagnosis, *Nucl Technol Radiat, 38* (2023), 2, pp. 125-134
[18] Kolacio, M. Š., *et al*., Validation of Two Calculation Options Built in Elekta Monaco Monte Carlo Based Algorithm Using MCNP Code, *Radiation Physics and Chemistry, 179* (2021), 109237
[19] Andreo, P., Monte Carlo Simulations in Radiotherapy Dosimetry, *Radiation Oncology, 13* (2018), 1
[20] Werner, C. J., *et al*., MCNP6. 2 Release Notes, Los Alamos National Laboratory, Report LA-UR-18-20808, 2018
[21] Brkić, H., *et al*., Influence of Head Cover on the Neutron Dose Equivalent in Monte Carlo Simulations of High Energy Medical Linear Accelerator, *Nucl Technol Radiat, 33* (2019), 2, pp. 217-222
[22] Brkić, H. *et al*., The Influence of Field Size and Off-Axis Distance on Photoneutron Spectra of the 18 MV Siemens Oncor Linear Accelerator Beam, *Radiation Measurements, 93* (2016), pp. 28-34
[23] Ivković, A., *et al*., The Influence of Shielding Reinforcement in a Vault with Limited Dimensions on the Neutron Dose Equivalent in Vicinity of Medical Electron Linear Accelerator, *Radiology and Oncology, 54* (2020), 2, pp. 247-252
[24] Ivković, A., *et al*., Accuracy of Empirical Formulas in Evaluation of Neutron Dose Equivalent Inside the $^{60}$Co Vaults Reconstructed for Medical Linear Accelerators, *International Journal of Radiation Research, 18* (2020), 1, pp. 99-107
[25] Detwiler, R., *et al*., Compendium of Material Composition Data for Radiation Transport Modeling, 2021
[26] Chadwick, M. B., *et al*., ENDF/B-VII. 0: Next Generation Evaluated Nuclear Data Library for Nuclear Science and Technology, *Nuclear Data Sheets, 107* (2006), 12, pp. 2931-3060
[27] ***, ICRP: Realistic Reference Phantoms: an ICRP/ICRU Joint Effort, A Report of Adult Reference Computational Phantoms, *Annals of the ICRP, 39* (2009), 2, pp. 1-164
[28] ***, ICRU: Neutron Interaction Data for Body Tissues, *ICRU Report, 46* (1992), pp. 1-8
[29] Forster, R. A., *et al*., Ten New Checks to Assess the Statistical Quality of Monte Carlo Solutions in MCNP1994
[30] Kaderka, R., *et al*., Out-Of-Field Dose Measurements in a Water Phantom Using Different Radiotherapy Modalities, *Physics in Medicine and Biology, 57* (2012), 16, pp. 5059-5074
[31] Filipev, I., *et al*., A Monte Carlo Study to Evaluate and Optimise the Angular Dependence of the Octa - A 2-D Silicon Array Detector Used for Dosimetry in Stereotactic Radiotherapy, *Radiation Measurements, 166* (2023), 106979
[32] Silva, E. H., *et al*., Energy and Angular Dependence of Radiophotoluminescent Glass Dosemeters for Eye Lens Dosimetry, *Radiation Protection Dosimetry, 170* (2016), 1-4, pp. 208-212
[33] Knežević, Ž., *et al*., Photon Dosimetry Methods Outside the Target Volume in Radiation Therapy: Optically Stimulated Luminescence (OSL), Thermoluminescence (TL) and Radiophotoluminescence (RPL) Dosimetry, *Radiation Measurements, 57* (2013), pp. 9-18
[34] Shine, N. S., *et al*., Out-of-Field Dose Calculation by a Commercial Treatment Planning System and Comparison by Monte Carlo Simulation for Varian TrueBeam®, *Journal of Medical Physics, 44* (2019), 3, p. 156

Received on August 13, 2024
Accepted on October 7, 2024

**Дарио ФАЈ, Хрвоје БРКИЋ, Вјекослав КОПАЧИН, Марија МАЈЕР, Жељка КНЕЖЕВИЋ, Свјетлана МАРИЋ, Младен КАСАБАШИЋ**

## МОНТЕ КАРЛО СИМУЛАЦИЈЕ ФОТОНСКЕ РАДИОТЕРАПИЈЕ ДОЈКЕ ТРУДНЕ ПАЦИЈЕНТКИЊЕ
### Карактеристике снопа

Сврха овога рада је да се опишу карактеристике енергетске и угаоне расподеле фотона током мегаволтне фотонске радиотерапије трудне пацијенткиње. Карактеристике фотона приказане су у циљаном волумену (дојка) и феталном положају, користећи Монте Карло симулације на антропоморфном фантому. Упоређене су карактеристике за различите материјале који се користе као замена ткива за израду физичких или рачунарских фантома. Средње енергије Тена супституцијских материјала разликују се до 10 % од ICRU референтних материјала. Фотонска средња енергија у феталном подручју значајно је нижа (више од 1 MeV) од оне у подручју дојке. Фотонска угаона дистрибуција на положају дојке има преферирани смер, док је тај смер на феталном положају распршен. Разлике у енергији фотона и угаоној расподели између мерних тачака у пољу зрачења и изван њега морају се узети у обзир за смањење несигурности мерења и добијања поузданих мерних података.

*Кључне речи: мегаволтно фотонско зрачење, Монте Карло симулација, карактеристика снопа, трудница*